

# LANDSAT-8 AS A PRECURSOR TO SENTINEL-2: OBSERVATIONS OF HUMAN IMPACTS IN COASTAL WATERS

Quinten Vanhellemont and Kevin Ruddick

Royal Belgian Institute of Natural Sciences (RBINS), Operational Directorate Natural Environment, Gulledele 100,  
1200 Brussels E-mail: [q.vanhellemont@mumm.ac.be](mailto:q.vanhellemont@mumm.ac.be)

## ABSTRACT

Satellite data have been frequently used for monitoring of suspended sediments and algal blooms in coastal waters. These waters are highly variable both in space and time, and with high resolution missions such as the currently operational Landsat-8 (15-30 m), and the soon to be launched Sentinel-2 (10-60 m), their small-scale spatial variability can be studied. Human impacts on suspended sediment distributions are much more apparent than at medium resolution. For example in Landsat-8 imagery, changes in sediment concentration are observed in the wakes of ships and associated with offshore constructions, such as wind turbine monopiles (Vanhellemont and Ruddick, 2014). Impacts of dredging activities are also observed. Based on the experience with Landsat-8, a number of new aquatic applications for Sentinel-2 have emerged.

## 1. INTRODUCTION

Satellite imagery has been used for mapping suspended sediments in coastal waters for several decades. Studies dating back to the seventies use high resolution imagery from the Landsat series of satellites (for example Amos and Alföldi, 1979; Rouse and Coleman, 1976). These satellites have a rather low revisit time (16 days track repeat with one satellite) and the Multi-Spectral Scanner (MSS) and its followers are generally quite noisy for marine applications.

Dedicated ocean colour satellites have been in low-earth orbit since the launch of SeaWiFS in 1997, and later MODIS on the Terra (1999) and Aqua (2002) platforms and MERIS on ENVISAT (2002). These first missions were more research oriented, and operationalization follows with VIIRS, launched in 2011 and Sentinel-3 that is to be launched mid-2015. These ocean colour sensors typically have wide swaths that allow frequent (often daily) revisits, 0.25 to 1 km spatial resolution and multiple sensitive spectral bands that allow for accurate atmospheric correction and water constituent retrieval.

With the launch of Landsat-8 in 2013, a NASA/USGS joint program, new high resolution (30 m) multispectral imagery with impressive signal-to-noise ratio became available free of charge (see band specifications in Table 1). First results using Landsat-8 are promising (Vanhellemont and Ruddick, 2014), and the sensor can be used to explore potential applications of the

upcoming Sentinel-2. The imager in Sentinel-2 will have a more extensive band set (Table 2), at several different resolutions including several bands with high potential for turbid water ocean colour applications. Here we present several Landsat-8 observations of direct human impacts on the coastal ecosystem in the southern Bight of the North Sea such as dredging activities and turbid wakes of ship and offshore constructions.

## 2. METHODS

Imagery from the Operational Land Imager (OLI) on Landsat-8 (L8) was acquired from EarthExplorer (<http://earthexplorer.usgs.gov/>). Rayleigh correction was performed using a lookup table generated with 6SV (Vermote et al., 2006). Rayleigh corrected RGB products were generated using bands 4, 3 and 2. Sharpening of the RGB imagery was performed by weighting the panchromatic 15 m resolution channel to the resampled visible channels:

$$f = \frac{3 \cdot L_{TOA}^8}{L_{TOA}^{2*} + L_{TOA}^{3*} + L_{TOA}^{4*}} \quad (1)$$

where  $L_{TOA}^{i*}$  is Top-of-Atmosphere radiance in band  $i$  rescaled to band 8 dimensions. The spatial variability in the panchromatic channel is represented by the scaling factor  $f$ , which is applied to the resampled RGB channels before composition. The sum of the spectral response of channels 2, 3 and 4 does not match that of the panchromatic channel, and a more rigorous merging should be performed for scientific application. Here the resampling is used solely for RGB image generation.

The aerosol correction was performed using bands 4 and 5 according to (Vanhellemont and Ruddick, 2014), by assuming a constant ratio of marine reflectances in those bands ( $\alpha = \rho_w^4 / \rho_w^5 = 8.7$ ) and a constant aerosol type ( $\epsilon$ ) over the scene. The aerosol type was determined as the median ratio of Rayleigh corrected reflectances ( $\rho_c^4 / \rho_c^5$ ) for clear water pixels in the scene. Clear water pixels were determined iteratively using a first guess of  $\epsilon = 1$  and a threshold on the resulting  $\rho_w^4$  ( $< 0.005$ ).

Suspended particulate matter concentration (SPM) is calculated using the generic multi-sensor algorithm of

(Nechad et al., 2010) applied to the marine reflectance in band 4 (655 nm):

$$SPM = \frac{A \rho_w}{1 - \rho_w / C} \quad (2)$$

where the tabulated values for 655 nm are used: A=289.29 gm<sup>-3</sup> and C=0.1686.

### 3. RESULTS

An OLI-derived map of suspended particulate matter concentration (SPM) for the Belgian and Dutch coastal zone around Zeebrugge and the Scheldt mouth is shown in Figure 1. Natural variability associated with the local bathymetry is observed at a high spatial resolution. For example, SPM on the shallow Vlakte van de Raan is higher than offshore. The small scale patterns on the northern side of the Vlakte van de Raan are linked to sand ripples on the seafloor, and similar features can also be seen elsewhere in the image. Near and in the port of Zeebrugge, as well as around the onshore breakwaters east of the harbour, small scale variability in sediment transport is observed. Large (>100m) container ships are present in the shipping lane to Antwerpen. These ships have a large draught and agitate bottom and near bed sediments, causing an increase of SPM in their wakes, which are up to several km long (see also Vanhellemont and Ruddick, 2014).

Near the harbour mouth of Zeebrugge, the turbid wake of a dredging vessel can be seen, with an associated dumping of dredged material. This cloud of dumped matter is black on the RGB image (Figure 2), and due to the absorbing properties of the matter, the single band SPM algorithm probably gives erroneous results (see lower SPM patch in Figure 1). The dumped matter was dredged from the harbour floor and the black colour is caused by high organic content and anoxic conditions. These harbour sediments are likely contaminated with pollutants, and in general higher concentrations of pollutants are found at the dumping sites (Van Hoey et al., 2012). A similar black plume of dumped sediments offshore of Oostende was found on a different image (Figure 3). On this image the effect of the dredging activities within the harbour are also clear: The water quality within the harbour, and of the outflowing water, is affected by the dredging operations. The disturbance of harbour sediments with dissolved or adsorbed pollutants can cause potential dispersal of pollutants (Bocchetti et al., 2008; Goossens and Zwolsman, 1996). In images without dredging activities, the colour of the water in and outside the harbour is comparable.

At offshore wind farms, which are typically constructed in near-shore, shallow waters with large tidal currents, effects on the SPM concentration are observed. In for

example the Thanet and London Array offshore wind farms (Figure 4), turbid wakes are observed associated with each turbine monopile (Vanhellemont and Ruddick, 2014). The wakes are aligned with tidal currents, and change every tide reversal. The tidal current and wakes in Figure 4 are approximately in the northward direction. The source of the sediments is as of now still unclear, but they are probably near-bed sediments or bottom sediments scoured up from around the base of the monopiles. The size of these wakes makes them impossible to detect on moderate resolution imagery, as their impact on the moderate resolution pixel signal is much less than natural variability in time and space. Moreover, the spatial structures themselves will be averaged to a level where these details cannot be observed.

### 4. CONCLUSIONS

Landsat-8 provides imagery of excellent quality, and shows promising results for coastal and inland water applications. At the native resolution of 30 m, human impacts on coastal waters are clear; changes in suspended sediments are found in the wakes of ships and offshore constructions, around ports and breakwaters. Dredging and dumping activities are observed, including actual dumping of the dredged materials and harbour outflows after dredging works. Simple calculations show that many of these small features are not separable from natural variability in a moderate resolution pixel. The moderate resolution sensors still have the big advantage of quick revisit times due to their large swath widths, and better signal-to-noise ratios for ocean colour applications.

Landsat-8 has shown several new applications where the resolution of typical ocean colour satellites is insufficient. These new applications will be further explored once Sentinel-2 is operational. A drawback of the high resolution sensors is the low temporal resolution, but the combination of the two data sources will allow for more frequent revisits. The swath of Sentinel-2 will be wider than Landsat-8, increasing temporal coverage.

### Acknowledgements

USGS/NASA are thanked for the Landsat-8 imagery. This work was performed for the FP-7 HIGHROC project (grant agreement n° 606797). Processing software was developed in the Belgian Science Policy Office JELLYFOR-BE project (SR/37/135).

### 5. REFERENCES

- Amos, C., Alföldi, T., 1979. The determination of suspended sediment concentration in a macrotidal system using Landsat data. *J. Sediment. Res.* 49, 159–173.

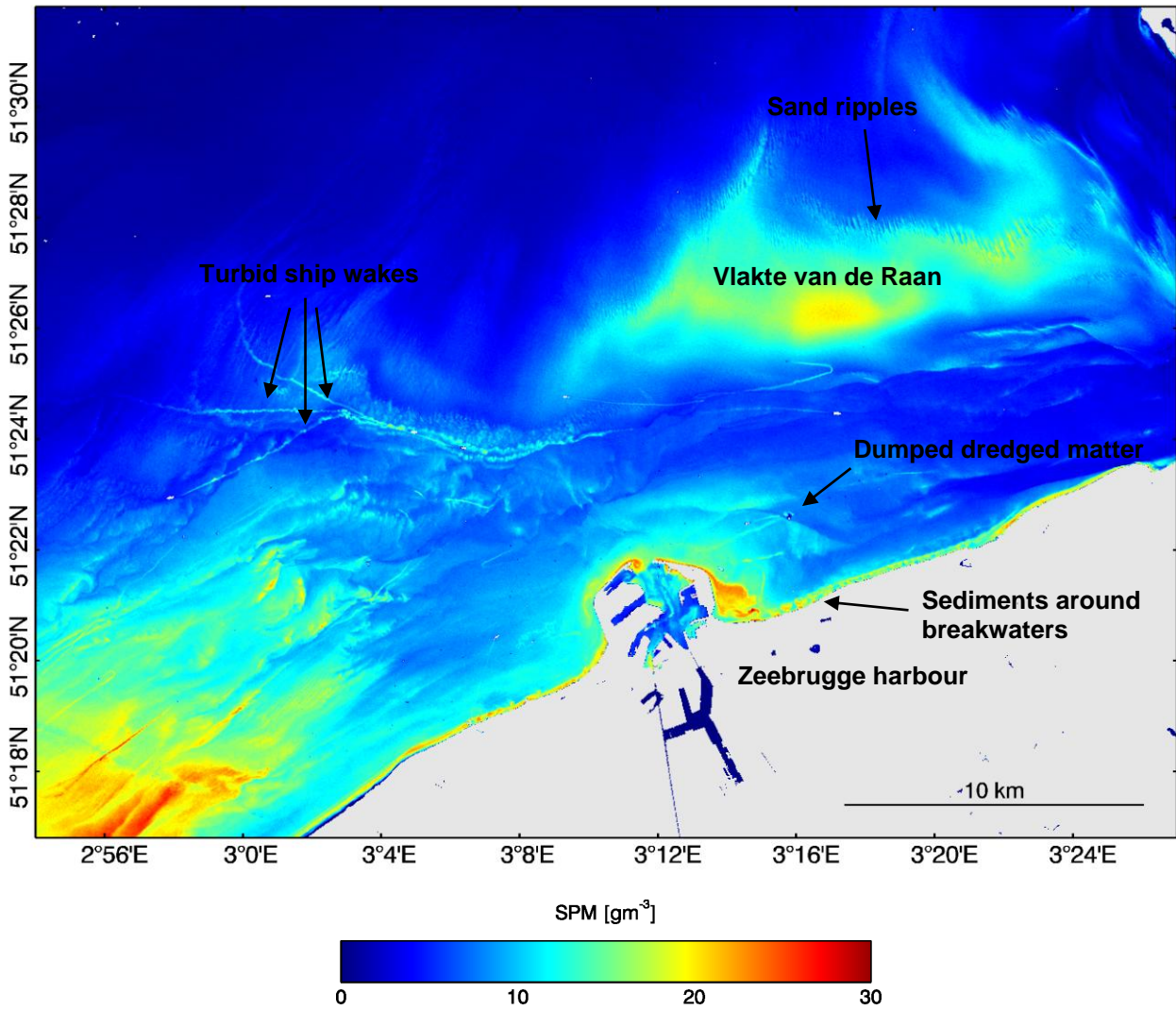
- Bocchetti, R., Fattorini, D., Pisanelli, B., Macchia, S., Oliviero, L., Pilato, F., Pellegrini, D., Regoli, F., 2008. Contaminant accumulation and biomarker responses in caged mussels, *Mytilus galloprovincialis*, to evaluate bioavailability and toxicological effects of remobilized chemicals during dredging and disposal operations in harbour areas. *Aquat. Toxicol.* 89, 257–266.
- Drusch, M., Gascon, F., Berger, M., 2010. GMES Sentinel-2 mission requirements document. ESA EOP-SM1163MR-Dr2 42.
- Goossens, H., Zwolsman, J.J., 1996. An evaluation of the behaviour of pollutants during dredging activities. *Terra Aqua* 20–28.
- Irons, J.R., Dwyer, J.L., Barsi, J.A., 2012. The next Landsat satellite: The Landsat Data Continuity Mission. *Remote Sens. Environ.* 122, 11–21.
- Nechad, B., Ruddick, K., Park, Y., 2010. Calibration and validation of a generic multisensor algorithm for mapping of total suspended matter in turbid waters. *Remote Sens. Environ.* 114, 854–866.
- Rouse, L.J., Coleman, J.M., 1976. Circulation observations in the Louisiana Bight using LANDSAT imagery. *Remote Sens. Environ.* 5, 55–66.
- Van Hoey, G., Delahaut, V., Derweduwen, J., Devriese, L., Dewitte, B., Hostens, K., Robbens, J., 2012. Biological and chemical effects of the disposal of dredged material in the Belgian Part of the North Sea (licensing period 2010-2011) 120.
- Vanhellemont, Q., Ruddick, K., 2014. Turbid wakes associated with offshore wind turbines observed with Landsat 8. *Remote Sens. Environ.* 145, 105–115.
- Vermote, E., Tanré, D., Deuzé, J., Herman, M., Morcrette, J., Kotchenova, S., 2006. Second simulation of a satellite signal in the solar spectrum-vector (6SV). 6S User Guide Version 3.

**Table 1** Bands of the Operational Land Imager (OLI) on Landsat-8, with wavelength range, ground sampling distance (GSD), signal-to-noise ratio (SNR) at reference radiance (Irons et al., 2012).

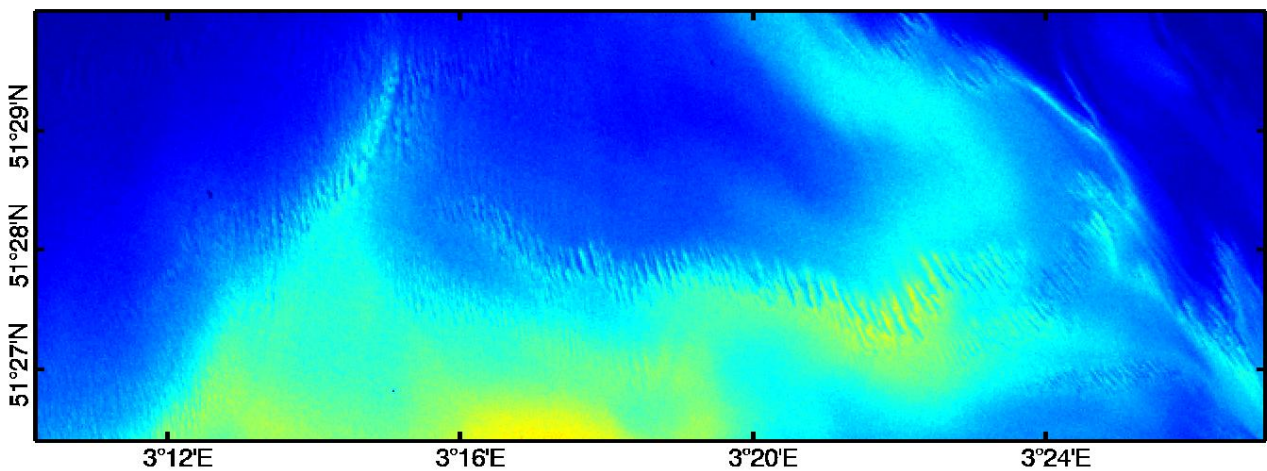
Band	Name	Wavelength (nm)	GSD (m)	SNR at reference L	reference L ( $W m^{-2} sr^{-1} \mu m^{-1}$ )
1	Coastal/Aerosol	433–453	30	232	40.0
2	Blue	450–515	30	355	40.0
3	Green	525–600	30	296	30.0
4	Red	630–680	30	222	22.0
5	NIR	845–885	30	199	14.0
6	SWIR 1	1560–1660	30	261	4.0
7	SWIR 2	2100–2300	30	326	1.7
8	PAN	500–680	15	146	23.0
9	CIRRUS	1360–1390	30	162	6.0

**Table 2** Bands of the MultiSpectral Imager (MSI) on Sentinel-2, with central wavelength and width, ground sampling distance (GSD), signal-to-noise ratio (SNR) at reference radiance (Drusch et al., 2010).

Band	Wavelength (nm)	Width (nm)	GSD (m)	SNR at reference L	reference L ( $W m^{-2} sr^{-1} \mu m^{-1}$ )
1	443	20	60	129	129.0
2	490	65	10	154	128.0
3	560	35	10	168	128.0
4	665	30	10	142	108.0
5	705	15	20	117	74.5
6	740	15	20	89	68.0
7	775	20	20	105	67.0
8	842	115	10	172	103.0
8b	865	20	20	72	52.5
9	940	20	60	114	9.0
10	1375	20	60	50	6.0
11	1610	90	20	100	4.0
12	2190	180	20	100	1.5



**Figure 1** Landsat-8/OLI-derived suspended matter concentration (SPM) for the Belgian coastal zone, 2013-09-05 at 10:42 UTC. Small scale features in the suspended sediment distribution can be observed, see text for details. The image below is a subset over the Vlakte van de Raan, showing the detailed SPM features associated with sand ripples.



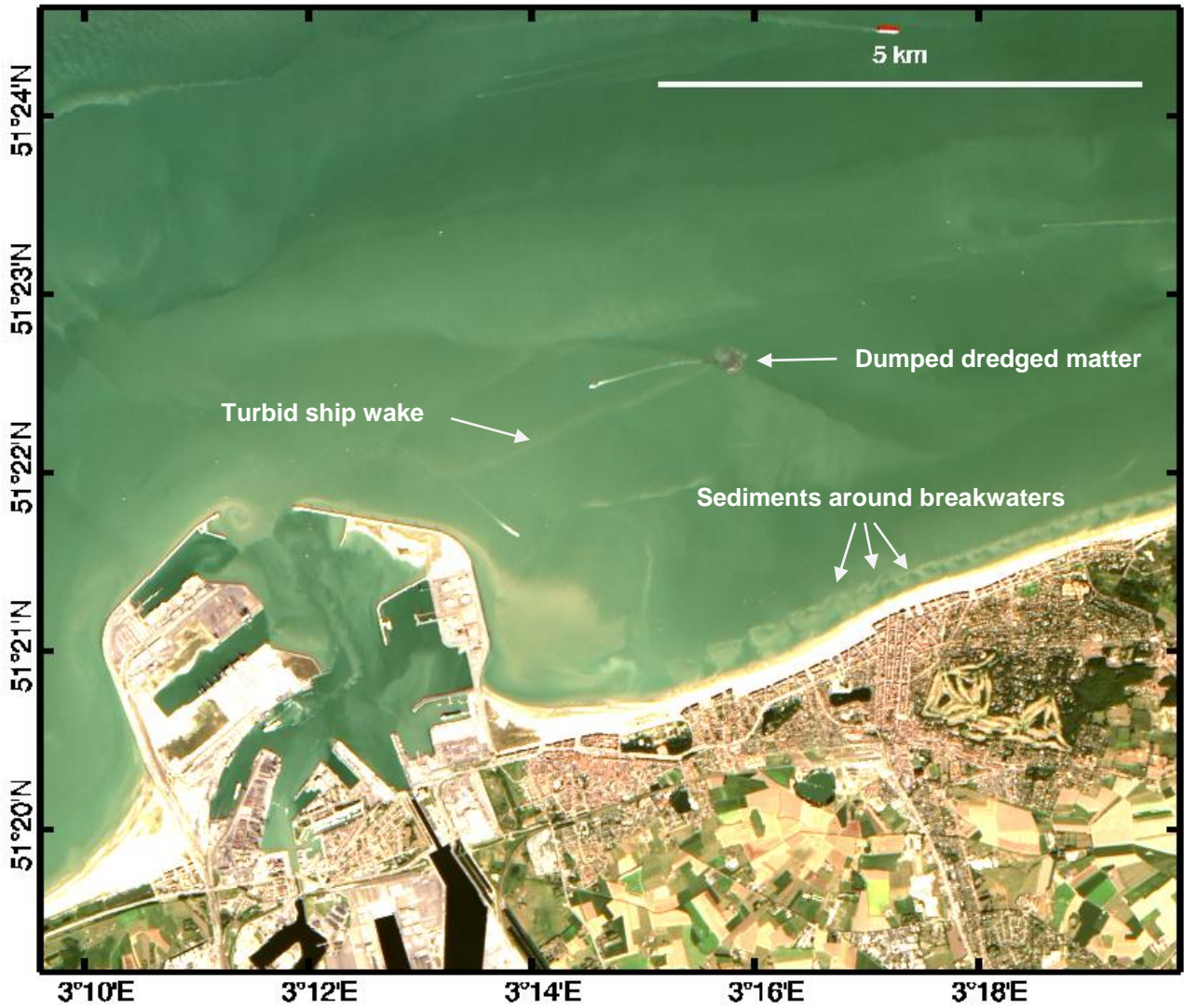


**Figure 2** Pan-sharpened Rayleigh corrected RGB for a subsene of Figure 1, showing the sediments in the harbour of Zeebrugge, a turbid wake of a dredging ship and a patch of dumped dredged matter. Sediment transport around the port and the breakwaters to the east can be seen.

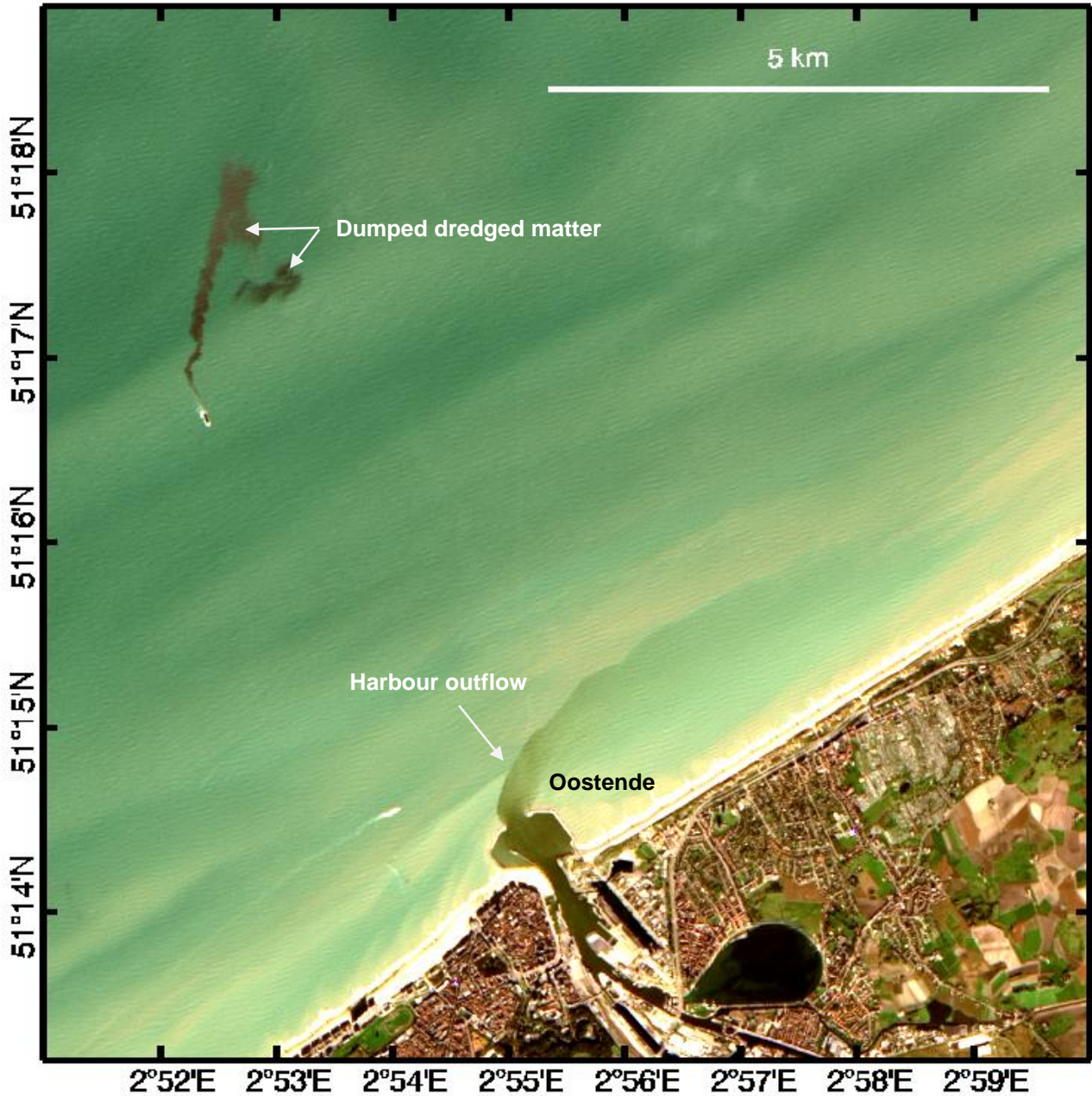


**Figure 3** Pan-sharpened Rayleigh corrected RGB of a dredger dumping material offshore of Oostende harbour, 2013-10-30 at 10:47 UTC. Surface wave features are taken over from the panchromatic channel (band 8).

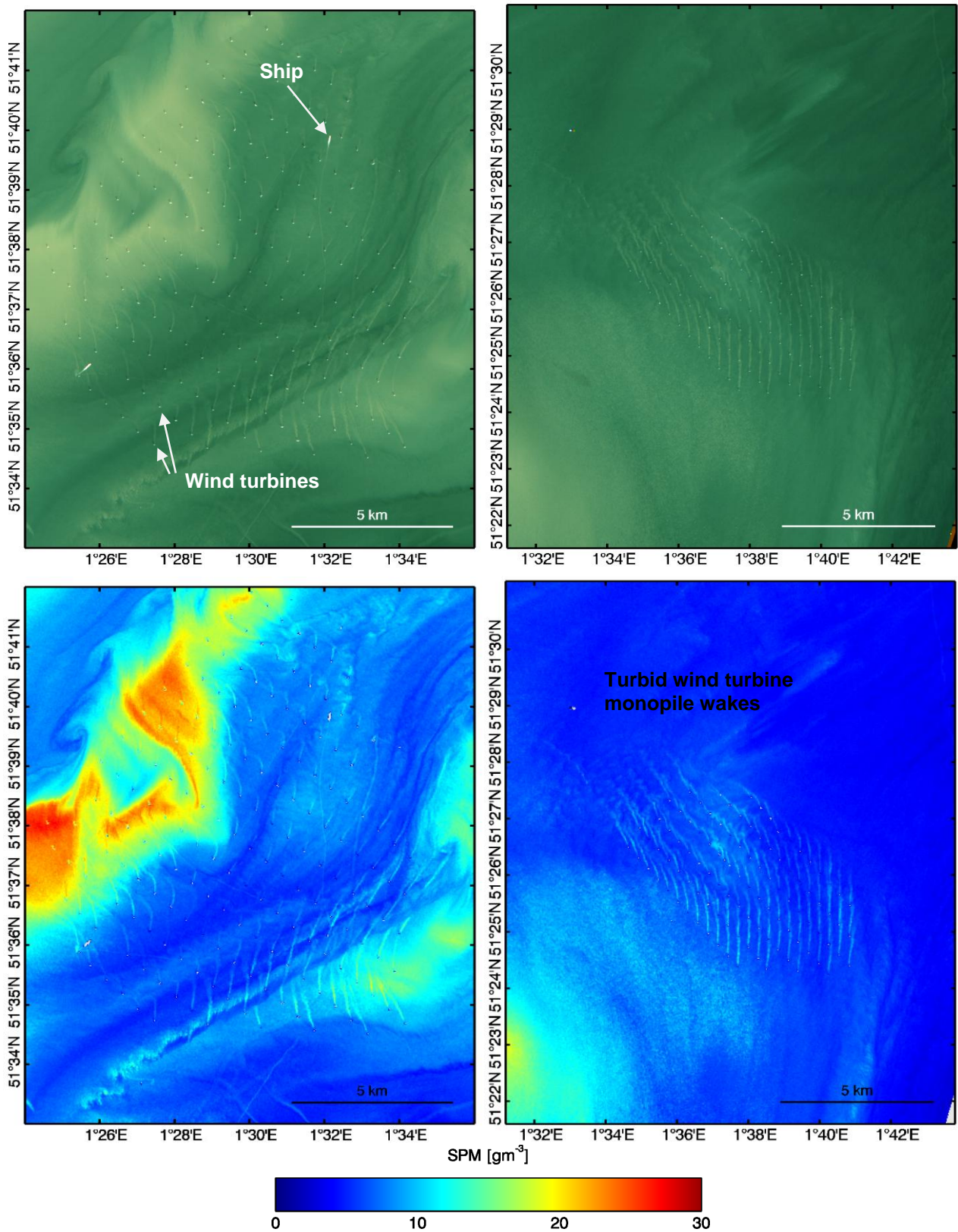


**Figure 4** Pan-sharpened Rayleigh corrected RGB (top) and suspended matter concentration (SPM, bottom) for the London Array (left) and Thanet (right) offshore wind farms on 2013-09-03 at 10:54 UTC. Higher SPM is found in the in-water wakes of the wind turbine monopiles and ships (results from Vanhellemont and Ruddick, 2014, © Elsevier).